Archives of Toxicology (2021) 95:3117–3131
https://doi.org/10.1007/s00204-021-03120-1

GENOTOXICITY AND CARCINOGENICITY

In vivo mutagenicity and tumor-promoting activity of 1,3-dichloro-2-propanol in the liver and kidneys of *gpt* delta rats

Kohei Matsushita[1] · Shinji Takasu[1] · Yuji Ishii[1] · Takeshi Toyoda[1] · Takanori Yamada[1,2] · Tomomi Morikawa[1] · Kumiko Ogawa[1]

Received: 28 June 2021 / Accepted: 7 July 2021 / Published online: 16 July 2021

Abstract

1,3-Dichloro-2-propanol (1,3-DCP), a food contaminant, exerts carcinogenic effects in multiple organs, including the liver and kidneys, in rats. However, the underlying mechanisms of 1,3-DCP-induced carcinogenesis remain unclear. Here, the in vivo mutagenicity and tumor-promoting activity of 1,3-DCP in the liver and kidneys were evaluated using medium-term *gpt* delta rat models previously established in our laboratory (GPG and GNP models). Six-week-old male F344 *gpt* delta rats were treated with 0 or 50 mg/kg body weight/day 1,3-DCP by gavage for 4 weeks. After 2 weeks of cessation, partial hepatectomy or unilateral nephrectomy was performed to collect samples for in vivo mutation assays, followed by single administration of diethylnitrosamine (DEN) for tumor initiation. One week after DEN injection, 1,3-DCP treatment was resumed, and tumor-promoting activity was evaluated in the residual liver or kidneys by histopathological analysis of preneoplastic lesions. *gpt* mutant frequencies increased in excised liver and kidney tissues following 1,3-DCP treatment. 1,3-DCP did not affect the development of glutathione *S*-transferase placental form-positive foci in residual liver tissues, but enhanced atypical tubule hyperplasia in residual kidney tissues. Detailed histopathological analyses revealed glomerular injury and increased cell proliferation of renal tubular cells in residual kidney tissues of rats treated with 1,3-DCP. These results suggested possible involvement of genotoxic mechanisms in 1,3-DCP-induced carcinogenesis in the liver and kidneys. In addition, we found that 1,3-DCP exhibited limited tumor-promoting activity in the liver, but enhanced clonal expansion in renal carcinogenesis via proliferation of renal tubular cells following glomerular injury.

Keywords 1,3-Dichloro-2-propanol · Food contaminant · *gpt* delta rat · In vivo mutagenicity · Reporter gene assay · Tumor promoting activity

Introduction

1,3-Dichloro-2-propanol (1,3-DCP; CAS No. 96-23-1) is a food contaminant formed under various conditions, including food processing, cooking, and storage (Williams et al. 2010). 1,3-DCP is contained in many foods and food ingredients, such as acid-hydrolyzed vegetable protein used as raw material for soy sauce and soy sauce-based products, malt products, cheese, meat products, and fish products, and the average of daily intake of 1,3-DCP is estimated as 0.09 µg/kg body weight (BW) to 0.136 µg/kg BW in the European Union and Australia (Andres et al. 2013). Thus, 1,3-DCP is a ubiquitous pollutant to which humans are exposed daily and may be difficult to avoid. In addition, because 1,3-DCP has been widely used as intermediate of epichlorohydrin production, a raw material used as various types of industrial products, occupational exposure of 1,3-DCP is also a safety concern for workers (NTP 2005).

In 2-year bioassays in rats, 1,3-DCP was found to show clear evidence of carcinogenicity in multiple organs, including the liver, kidneys, thyroid, and tongue (NTP 2005). 1,3-DCP showed positive results in various types of in vitro genotoxicity assays, such as Ames tests and sister chromatid exchange tests, whereas negative results were reported in two in vivo genotoxicity assays, i.e., rat bone marrow micronucleus assays and rat hepatocyte

✉ Kohei Matsushita
k-matsushita@nihs.go.jp

[1] Division of Pathology, National Institute of Health Sciences, 3-25-26 Tonomachi, Kawasaki, Kanagawa 210-9501, Japan

[2] Laboratory of Veterinary Pathology, Tokyo University of Agriculture and Technology, 3-5-8 Saiwai-cho, Fuchu, Tokyo 183-8509, Japan

unscheduled DNA synthesis assays (NTP 2005). At the 67th meeting of the Joint Food and Agricultural Organization (FAO)/World Health Organization (WHO) Expert Committee on Food Additives (JECFA), 1,3-DCP was evaluated as a food contaminant and judged as low concern for human health based on the margin of exposure (JECFA 2006). In this meeting, JECFA concluded that the critical effect of 1,3-DCP is carcinogenicity and that it is inappropriate to estimate a tolerable intake level, because genotoxic mechanisms could not be excluded given the positive results of in vitro genotoxicity assays and multiplicity for target organs of 1,3-DCP-induced carcinogenesis. However, no studies have demonstrated that 1,3-DCP exerts genotoxic effects in target organs for carcinogenicity. Therefore, clarifying whether genotoxic mechanisms are involved in target organs of 1,3-DCP-induced carcinogenesis may be helpful for consolidation of evidence for safety assessments.

gpt delta rats, transgenic rats carrying a reporter gene, have been developed to evaluate the genotoxicity of chemicals in whole body organs (Nohmi 2016). Reporter gene mutation assays using *gpt* delta rats can be conducted under the same conditions used for general toxicity or carcinogenicity studies, enabling us to simultaneously evaluate other parameters related to carcinogenesis, such as DNA modifications, enzyme induction, and cell proliferation (Hibi et al. 2017; Ishii et al. 2019a, b; Jin et al. 2013). Accordingly, we developed medium-term in vivo systems using *gpt* delta rats for analysis of the underlying mechanisms of carcinogens in the liver and kidneys, named the GPG and GNP models, respectively (Matsushita et al. 2013, 2014, 2015). In these models, partial hepatectomy (PH) or unilateral nephrectomy (UN) were performed after 4 weeks of test chemical treatment to collect samples for in vivo mutation assays. Diethylnitrosamine (DEN) was administered after PH or UN to initiate hepato- or renal carcinogenesis followed by test chemical treatment. The tumor-promoting activity of test chemicals was evaluated by histopathological analysis for preneoplastic lesions in residual liver or kidney tissues. Because two critical endpoints involved in carcinogenesis, i.e., in vivo mutagenicity and tumor-promoting activity, can be evaluated independently in a single study, these models are promising models for precise evaluation of the mechanisms of chemical carcinogenesis.

The purpose of the current study was to evaluate the in vivo mutagenicity and tumor-promoting activity of 1,3-DCP in the liver and kidneys of GPG and GNP model rats, respectively. In addition, the general toxicological profiles of 1,3-DCP in wild-type F344 male rats were assessed in a preliminary 4-week repeated dose study performed to determine of the dosage of 1,3-DCP in GPG and GNP models.

Materials and methods

Chemicals

1,3-DCP and aristolochic acid (AA) were obtained from Sigma-Aldrich (St. Louis, MO, USA). DEN and estragole (ES) were purchased from Tokyo Chemical Industry (Tokyo, Japan).

Experimental animals and housing conditions

Five-week-old male specific pathogen-free F344/NSlc rats and F344/NSlc-Tg (*gpt* delta) rats carrying approximately five tandem copies of the transgene lambda EG10 per haploid genome were obtained from Japan SLC (Shizuoka, Japan) and acclimated for 1 week prior to testing. The animals were housed in polycarbonate cages with soft chip bedding (Sankyo Labo Service, Tokyo, Japan) in a room with a barrier system and a controlled light/dark cycle (12 h), ventilation (air-exchange rate 20 times/h), temperature (23 ± 1 °C), and relative humidity ($50\% \pm 5\%$) during the study. Each animal had free access to tap water and a basal diet (CRF-1; Oriental Yeast Co., Ltd., Tokyo, Japan). At the end of each experiment, the rats were euthanized by exsanguination via transection of the abdominal aorta under deep anesthesia by inhalation of isoflurane. The protocols for the animal experiment were approved by the Animal Care and Utilization Committee of the National Institute of Health Sciences.

Animal treatment

Experiment 1

Six-week-old male F344 rats were given distilled water (vehicle) or 25, 50, or 100 mg/kg (10 mL/kg) 1,3-DCP by gavage once a day for 4 weeks ($n = 5$). General conditions and mortality were checked daily. Body weights and amount of supplied and residual diet were measured twice a week. All rats that survived during the experimental period were fasted overnight at the completion of the treatment, and blood samples were collected from the abdominal aorta under deep anesthesia, caused by inhalation of isoflurane, for hematology and serum biochemistry. Complete necropsy was performed for animals in the 0, 25, and 50 mg/kg groups, which were sacrificed the day after the final administration. The brain, thymus, heart, lungs, spleen, liver, kidneys, adrenal glands, testes, seminal vesicles, prostate, pituitary, and thyroid (including parathyroid) were weighed. These organs and the following tissues were fixed in 10% neutral buffered formalin, and paraffin-embedded sections

were prepared and stained with hematoxylin and eosin (HE) for histopathological examination: skin, mammary gland, sternum with marrow, femur with marrow, mandibular and mesenteric lymph nodes, salivary glands, aorta, trachea, tongue, esophagus, stomach, small and large intestines, pancreas, urinary bladder, epididymides, seminal vesicles, prostate gland, spinal cord with vertebrae, trigeminal nerve, sciatic nerve, harderian glands, femoral skeletal muscle, and nasal cavity. The testes and eyes were fixed in Bouin's fixative and Davidson's solution, respectively. Bony tissues, including the nasal cavity, vertebrae, sternum, and femur, were decalcified with a mixture of 10% formic acid and 10% buffered formalin for up to 2 weeks. Additional immunohistochemical analysis was performed using formalin-fixed liver samples of the sacrificed animals. A portion of liver samples of the sacrificed animals was also stored at − 80 °C for western blotting, reverse transcription quantitative polymerase chain reaction (RT-qPCR), and measurement of 8-hydroxy-2′-deoxyguanosine (8-OHdG). In the 100 mg/kg group, animals showing poor general condition were sacrificed under deep anesthesia by isoflurane, and animals found dead were necropsied immediately after detection. Systemic organs of dead/moribund sacrificed animals were also sampled and fixed in 10% neutral buffered formalin. Histopathological assessment was performed on all tissues in the 0, 50, and 100 mg/kg groups and on liver and nasal cavity tissues in the 25 mg/kg group.

Experiment 2

The experimental protocol for GPG model is described in Fig. 1A. Six-week-old male F344 *gpt* delta rats were given distilled water or 50 mg/kg 1,3-DCP by gavage once a day ($n = 15$). The dose of 1,3-DCP was determined based on the results of experiment 1. The rats in the positive control group for the GPG model were given 150 mg/kg (10 mL/kg) ES, a genotoxic hepatocarcinogen, by gavage once a day ($n = 15$). After 4 weeks, test chemical administration was interrupted in all animals. At 6 weeks, PH was performed in all rats under deep anesthesia by isoflurane, and the excised liver tissues were perfused with saline to remove residual blood and stored at − 80 °C for *gpt* assays. An intraperitoneal injection of DEN at a dose of 10 mg/kg was administered at 18 h after PH to initiate hepatocarcinogenesis. The washout period of test chemical treatment was set to avoid interaction between the test chemical and DEN. Test chemical treatment resumed at 7 weeks. At 13 weeks, animals were sacrificed, and a portion of the residual liver sample

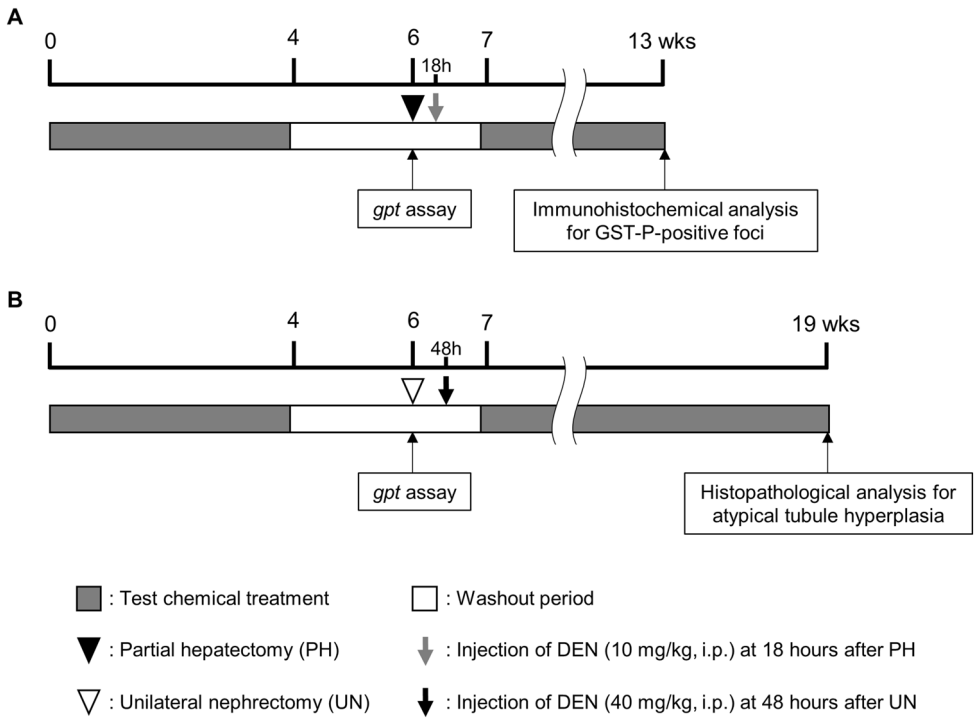

Fig. 1 Standard protocols for the medium-term *gpt* delta rat model for analysis of hepato- and renal carcinogenesis and the underlying mode of action. Animals were 6-week-old male F344 *gpt* delta rats. **A** In the GPG model, *gpt* assays were performed in excised liver samples as an indicator of in vivo mutagenicity. Tumor-promoting activities were evaluated based on the enhancement of glutathione *S*-transferase placental form (GST-P)-positive foci, preneoplastic lesions of hepatocytes, induced by diethylnitrosamine (DEN) in residual liver samples. **B** In the GNP model, *gpt* assays were performed in excised kidney samples. Tumor-promoting activities were evaluated based on enhancement of atypical tubule hyperplasia, preneoplastic lesions of renal cells, induced by DEN in residual kidney samples

was fixed in 10% neutral buffered formalin for histopathological and immunohistochemical analysis. The effects of test chemical exposure on the development of DEN-induced glutathione *S*-transferase placental form (GST-P)-positive foci, a well-established preneoplastic marker in the rat liver (Tsuda et al. 2010), were analyzed by immunohistochemistry to evaluate tumor-promoting activity. The number and area of GST-P-positive foci consisting of five or more nucleated hepatocytes in a cross section were evaluated using an image analyzer (HALO, Albuquerque, NM, USA). Another portion of residual liver tissue was stored − 80 °C for qPCR.

Experiment 3

The experimental protocol for GNP model is described in Fig. 1B. Six-week-old male F344 *gpt* delta rats were given distilled water or 50 mg/kg 1,3-DCP by gavage once a day ($n = 15$). The rats in the positive control group for the GNP model were given 0.3 mg/kg (10 mL/kg) AA, a genotoxic renal carcinogen, by gavage once a day ($n = 15$). After 4 weeks, test chemical administration was interrupted in all animals. At 6 weeks, UN was performed in all rats under deep anesthesia by isoflurane, and the excised kidney tissues were perfused with saline to remove residual blood and stored at − 80 °C for *gpt* assay. An intraperitoneal injection of DEN at a dose of 40 mg/kg was administered at 48 h after UN to initiate renal carcinogenesis. Test chemical treatment resumed at 7 weeks. At 19 weeks, animals were sacrificed, and a portion of the residual kidney sample was fixed in 10% neutral buffered formalin for histopathological and immunohistochemical analysis. The effects of test chemical exposure on the development of atypical tubule hyperplasia, preneoplastic lesions of renal cells (Frazier et al. 2012), were analyzed by histopathological examination to evaluate tumor-promoting activity. In addition, Periodic Acid-Schiff (PAS) staining was performed to assess glomerular injury. A portion of the residual kidney tissue was also stored − 80 °C for qPCR.

Hematology and serum biochemistry

In experiment 1, the following hematological parameters were analyzed using a ProCyte Dx automatic hematology analyzer (IDEXX Laboratories, Westbrook, ME, USA): white blood cell count (WBC), red blood cell count (RBC), hemoglobin concentration (HGB), hematocrit (HCT), mean corpuscular volume (MCV), mean corpuscular hemoglobin (MCH), mean corpuscular hemoglobin concentration (MCHC), reticulocyte count (RET), and platelet count (PLT). Serum biochemical analysis of the following parameters was performed by SRL (Tokyo, Japan): total protein (TP), albumin (ALB), albumin/globulin ratio (A/G), blood urea nitrogen (BUN), creatinine (CRE), sodium (Na), potassium (K), chlorine (Cl), calcium (Ca), inorganic phosphorus (IP), aspartate aminotransferase (AST), alanine aminotransferase (ALT), alkaline phosphatase (ALP), γ-glutamyl transpeptidase (γ-GTP), total cholesterol (T-CHO), triglyceride (TG), total bilirubin (T-BIL), and glucose (GLU).

Immunohistochemistry

For immunohistochemistry, sections were immersed in 3% H_2O_2/methanol for inactivation of endogenous peroxidase activity. The following primary antibodies were used: rabbit polyclonal antibodies against cleaved-caspase (c-caspase) 3 (1:400 dilution; Cell Signaling Technology, Danvers, MA, USA), rabbit polyclonal antibodies against GST-P (1:1000 dilution; Medical and Biological Laboratories Co., Ltd., Nagoya, Japan), and rabbit polyclonal antibodies against Ki67 (1:500 dilution; Abcam, Cambridge, UK). Antigen retrieval for c-caspase 3 and Ki67 was performed in pH 9.0 antigen retrieval solution (Dako, Glostrup, Denmark) and pH 6.0 citrate buffer, respectively, using an autoclave for 15 min at 121 °C. After blocking of nonspecific reactions with 10% normal goat serum, the sections were incubated with each primary antibody overnight at 4 °C. Visualization was performed using a Histofine Simple Stain Rat MAX PO kit (Nichirei Corporation, Tokyo, Japan) and 3,3′-diaminobenzidine. All c-caspase 3-positive cells in liver sections were counted, and the numbers of positive cells per unit area of liver were calculated. At least 4000 intact hepatocytes in the liver and renal cells in the kidney per animal were counted, and labeling indices were calculated as the percentages of cells staining positive for Ki67.

Western blotting

In experiment 1, the livers from rats were homogenized, and the resulting supernatants were used. Samples were separated by sodium dodecyl sulfate polyacrylamide gel electrophoresis and transferred to 0.45-μm polyvinylidene difluoride membranes (Millipore, Billerica, MA, USA). For detection of target proteins, rabbit polyclonal antibodies against GST-P (1:1000 dilution; Medical and Biological Laboratories) were used. Membranes were incubated with primary antibodies overnight at 4 °C and secondary antibodies (Cell Signaling Technology) for 60 min at room temperature. Protein detection was facilitated by chemiluminescence using ECL Prime (GE Healthcare Japan Ltd., Tokyo, Japan).

qPCR for analysis of mRNA expression

Total RNA was extracted from liver and kidney tissues using an RNeasy Mini Kit (Qiagen K.K., Tokyo, Japan) according to the manufacturer's instructions. cDNA copies of total

RNA were obtained using a High-Capacity cDNA Reverse Transcription kit (Thermo Fischer Scientific, Waltham, MA, USA).

All PCR assays were performed with primers for rat *Ccnd1* (Rn00432359_m1), *Ccne1* (Rn01457762_m1), *Ccna2* (Rn01493715_m1), *Ccnb1* (Rn01494180_g1), and *Gstp1* (Rn00561378_gH) purchased from Agilent Technologies (Santa Clara, CA, USA) to evaluate mRNA expression of cyclin D1, cyclin E1, cyclin A2, cyclin B1, and GST-P. TaqMan Rodent GAPDH Control Reagents were used as an endogenous reference. PCR was carried out using a QuantStudio 3 Real-Time PCR System (Applied Biosystems, Waltham, MA, USA) with TaqMan Fast Universal PCR Master Mix and TaqMan Gene Expression Assays (Life Technologies, Carlsbad, CA, USA). The expression levels of target genes were calculated according to the relative standard curve method and were determined by normalization to *Gapdh* expression. Data were presented as fold-change values of samples in the control group compared with those in the 1,3-DCP treatment groups.

Measurement of 8-OHdG

In experiment 1, livers of scheduled sacrificed animals were used for the measurement of 8-OHdG. DNA was extracted and digested as described previously (Umemura et al. 2003). Briefly, nuclear DNA was extracted with a DNA Extractor WB Kit (Wako Pure Chemical Industries, Osaka, Japan). For further prevention of artifactual oxidation in the cell lysis step, deferoxamine mesylate (Sigma-Aldrich) was added to the lysis buffer. The DNA was digested to deoxynucleotides by treatment with nuclease P1 and alkaline phosphatase, using an 8-OHdG Assay Preparation Reagent Set (Wako Pure Chemical Industries). The levels of 8-OHdG (8-OHdG/10^5 dG) were measured by high-performance liquid chromatography with an electrochemical detection system (Coulochem II; ESA, Bedford, MA, USA) as previously reported (Umemura et al. 2006).

In vivo mutation assay

6-Thioguanine (6-TG) was used according to previously described methods (Nohmi et al. 2000). Briefly, genomic DNA was extracted from liver and kidney samples, and lambda EG10 DNA (48 kb) was then rescued in phages by in vitro packaging. For 6-TG selection, the packaged phages were incubated with *Escherichia coli* YG6020, which expresses Cre recombinase, and converted to plasmids carrying genes encoding *gpt* and chloramphenicol acetyltransferase. The infected cells were mixed with molten soft agar and poured onto agar plates containing chloramphenicol and 6-TG. To determine the total number of rescued plasmids, the infected cells were poured on plates containing chloramphenicol without 6-TG. The plates were incubated at 37 °C for the selection of 6-TG-resistant colonies. Positive colonies were counted on day 3 and collected on day 4. The *gpt* mutant frequencies (MFs) were calculated by dividing the number of *gpt* mutants by the number of rescued phages.

Statistical analysis

Statistical analysis was performed using GraphPad Prism 9 (GraphPad Software, Inc., San Diego, CA, USA). In experiment 1, variances in the data for body weights during the experiment as well as hematologic values, serum biochemistry, organ weight values (both absolute and relative weights), numbers of c-caspase 3-positive cells, Ki67-positive indices, 8-OHdG levels, and mRNA expression levels in the liver were evaluated using analysis of variance, followed by Dunnett's multiple comparison test to compare with data in the control group.

In experiments 2 and 3, the data for *gpt* assays, quantitative analysis of GST-P-positive foci and preneoplastic lesions of renal cells, numbers of Ki67-positive indices, and mRNA expression levels were analyzed by *t* tests for comparisons with data in the control group. Differences with p values less than 0.05 were considered statistically significant.

Results

Experiment 1

In-life parameters

In the 100 mg/kg group, four rats were found dead, and one rat was sacrificed due to marked worsening of general condition on the morning of day 2. All animals in the 0, 25, and 50 mg/kg groups survived until the scheduled necropsy, and there were no clinical signs related to administration of 1,3-DCP. No obvious changes in body weight and food intake were observed in the 25 and 50 mg/kg groups compared with the control group (Fig. 2).

Hematology and serum biochemistry

Hematology data are summarized in Table 1. In the 25 and 50 mg/kg groups, significant fluctuations in parameters suggesting anemia, including decreases in RBC, HGB, HCT, MHC, and MCHC and an increase in RET, were considered to be adverse effects of 1,3-DCP. Data for serum biochemistry are summarized in Table 2. Serum ALT and ALB were significantly increased in the 50 mg/kg group. A significant decrease in TG was observed in the 25 and 50 mg/kg groups. These fluctuations were considered to be related to

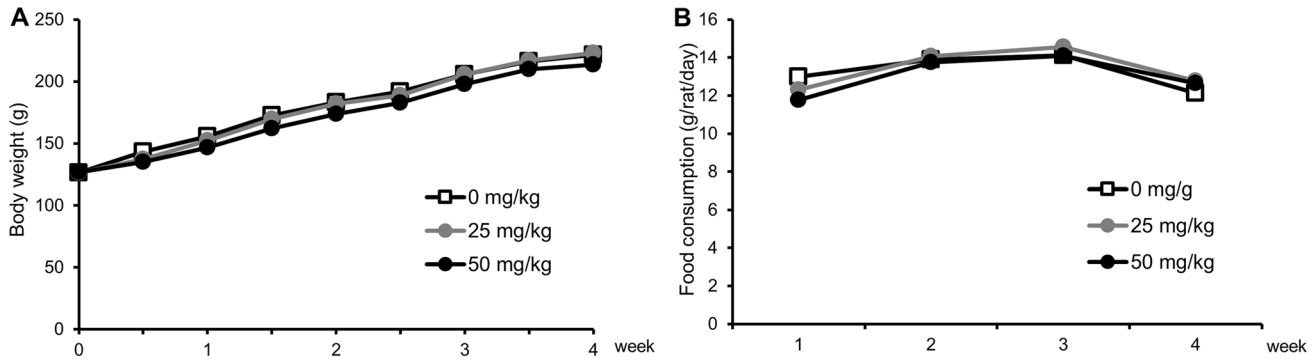

Fig. 2 Body weights and food consumption in a preliminary dose-finding study using wild-type F344 rats. The data for body weights and food consumption in the 100 mg/kg group were excluded, because all animals died or were moribund sacrificed following single administration. **A** Body weights were not changed in rats treated with 25 and 50 mg/kg 1,3-DCP compared with the control group during the experiment. **B** There were no obvious effects on food consumption following 1,3-DCP treatment

Table 1 Hematological data in a preliminary 4-week repeated dose oral toxicity study

	0 mg/kg	25 mg/kg	50 mg/kg
No. of animals examined	5	5	5
RBC ($\times 10^6$/μL)	8.7 ± 0.1	8.2 ± 0.2**	8.5 ± 0.1*
HGB (g/dL)	15.4 ± 0.1	14.2 ± 0.2**	14.5 ± 0.2**
HCT (%)	45.9 ± 0.4	43.3 ± 0.7**	44.4 ± 0.7**
MCV (fL)	52.6 ± 0.2	52.6 ± 0.8	52.2 ± 0.2
MHC (pg)	17.6 ± 0.2	17.2 ± 0.1**	17.1 ± 0.1*
MCHC (g/dL)	33.5 ± 0.2	32.9 ± 0.4*	32.7 ± 0.3*
RET (%)	3.20 ± 0.23	3.77 ± 0.36*	3.79 ± 0.32*
PLT ($\times 10^3$/μL)	795.8 ± 43.8	777.4 ± 46.0	784.6 ± 36.9
WBC ($\times 10^2$/μL)	37.2 ± 7.6	31.1 ± 2.9	37.0 ± 6.6
Differential leukocyte counts			
Neutrophils ($\times 10^2$/μL)	7.5 ± 1.8	5.2 ± 0.5	6.2 ± 0.9
Lymphocytes ($\times 10^2$/μL)	28.5 ± 6.6	24.9 ± 2.7	29.6 ± 5.4
Monocytes ($\times 10^2$/μL)	0.8 ± 0.3	0.7 ± 0.1	0.8 ± 0.2
Eosinophils ($\times 10^2$/μL)	0.3 ± 0.1	0.3 ± 0.1	0.4 ± 0.2
Basophils ($\times 10^2$/μL)	0.1 ± 0.1	0.1 ± 0.1	0.1 ± 0.1

Values are means ± standard deviations

*, **Significantly different from the 0 mg/kg group at $p < 0.05$, 0.01, respectively

Table 2 Serum biochemical data in a preliminary 4-week repeated dose oral toxicity study

	0 mg/kg	25 mg/kg	50 mg/kg
No. of animals exained	5	5	5
TP (g/dL)	6.0 ± 0.1	6.2 ± 0.2	6.3 ± 0.3
ALB (g/dL)	4.4 ± 0.1	4.5 ± 0.1	4.6 ± 0.1*
A/G	2.6 ± 0.2	2.6 ± 0.1	2.7 ± 0.2
BUN (mg/dL)	19.5 ± 1.5	17.3 ± 0.6*	17.8 ± 1.5
CRE (mg/dL)	0.25 ± 0.02	0.22 ± 0.02*	0.21 ± 0.01*
Na (mEq/L)	144.0 ± 0.0	144.2 ± 1.1	144.0 ± 0.7
K (mEq/L)	4.66 ± 0.18	4.48 ± 0.16	4.56 ± 0.18
Cl (mEq/L)	101.2 ± 1.8	100.2 ± 1.1	101.0 ± 1.7
Ca (mg/dL)	10.0 ± 0.2	10.4 ± 0.2*	10.3 ± 0.2
IP (mg/dL)	6.7 ± 0.3	7.2 ± 0.2	6.8 ± 0.4
AST (IU/L)	101.0 ± 9.1	84.0 ± 12.1	97.0 ± 16.8
ALT (IU/L)	42.4 ± 1.82	38.8 ± 5.07	50.6 ± 5.46*
ALP (IU/L)	785.2 ± 48.3	645.4 ± 42.2**	650.6 ± 31.2*
γ-GTP (IU/L)	3 >	3 >	3 >
T-CHO (mg/dL)	58.8 ± 1.5	61.4 ± 3.4	56.6 ± 5.3
TG (mg/dL)	54.8 ± 5.9	36.0 ± 10.4*	33.8 ± 15.1*
T-BIL (mg/dL)	0.03 ± 0.01	0.01 ± 0.02	0.03 ± 0.01
GLU (mg/dL)	111.8 ± 10.0	129.2 ± 20.4	116.8 ± 30.6

Values are mean ± standard deviations

*, **Significantly different from the 0 mg/kg group at $p < 0.05$, 0.01, respectively

hepatotoxicity of 1,3-DCP. Significant changes observed in other parameters were considered to have no toxicological significance, because the changes were the opposite of the toxicological changes or showed no dose dependency.

Organ weights

Data for final BWs and organ weights are shown in Table 3. Significant increases in absolute and relative liver weights and relative kidney weights were observed in the 25 and 50 mg/kg groups. Although absolute and relative spleen weights were significantly increased in the 25 mg/kg group, the changes showed no dose dependency.

Necropsy and histopathology

At necropsy, hemorrhage from the nose and mottled white foci in the liver were observed in dead or moribund sacrificed animals in the 100 mg/kg group. There were no

Table 3 Organ weights in a preliminary 4-week repeated dose oral toxicity study

	0 mg/kg	25 mg/kg	50 mg/kg
No. of animals examined	5	5	5
Final body weight (g)	205.5 ± 4.2	205.5 ± 7.0	196.4 ± 7.1
Absolute			
Brain (g)	1.81 ± 0.03	1.78 ± 0.05	1.77 ± 0.05
Thymus (g)	0.29 ± 0.02	0.33 ± 0.02	0.33 ± 0.01
Heart (g)	0.67 ± 0.01	0.66 ± 0.05	0.64 ± 0.04
Spleen (g)	0.47 ± 0.01	0.52 ± 0.02**	0.48 ± 0.03
Liver (g)	5.70 ± 0.12	7.26 ± 0.29**	7.50 ± 0.20**
Adrenals (mg)	33.5 ± 3.75	34.0 ± 0.59	34.3 ± 2.59
Kidneys (g)	1.46 ± 0.08	1.61 ± 0.05	1.57 ± 0.12
Testes (g)	2.53 ± 0.07	2.56 ± 0.12	2.49 ± 0.09
Lungs (g)	0.77 ± 0.03	0.81 ± 0.09	0.78 ± 0.05
Pituitary (mg)	7.56 ± 0.74	8.24 ± 0.50	7.90 ± 0.62
Thyroid (mg)	14.2 ± 1.84	14.2 ± 0.83	13.8 ± 0.97
Salivary gland (g)	0.42 ± 0.01	0.42 ± 0.02	0.41 ± 0.04
Seminal vesicle (g)	0.54 ± 0.17	0.52 ± 0.05	0.48 ± 0.10
Prostate (g)	0.42 ± 0.03	0.43 ± 0.06	0.36 ± 0.07
Relative			
Brain (g/100 g BW)	0.89 ± 0.01	0.87 ± 0.03	0.90 ± 0.02
Thymus (g/100 g BW)	0.14 ± 0.01	0.16 ± 0.01	0.16 ± 0.01
Heart (g/100 g BW)	0.32 ± 0.01	0.32 ± 0.01	0.33 ± 0.02
Spleen (g/100 g BW)	0.23 ± 0.01	0.25 ± 0.02*	0.24 ± 0.01
Liver (g/100 g BW)	2.78 ± 0.07	3.53 ± 0.10**	3.82 ± 0.07**
Adrenals (mg/100 g BW)	16.3 ± 1.53	16.6 ± 0.68	17.5 ± 1.39
Kidneys (g/100 g BW)	0.71 ± 0.03	0.78 ± 0.03**	0.80 ± 0.05**
Testes (g/100 g BW)	1.23 ± 0.02	1.25 ± 0.06	1.27 ± 0.02
Lungs (g/100 g BW)	0.38 ± 0.01	0.40 ± 0.04	0.40 ± 0.02
Pituitary (mg/100 g BW)	3.68 ± 0.31	4.02 ± 0.33	4.02 ± 0.32
Thyroid (mg/100 g BW)	6.92 ± 0.82	6.92 ± 0.43	7.02 ± 0.60
Salivary gland (g/100 g BW)	0.20 ± 0.01	0.20 ± 0.01	0.21 ± 0.02
Seminal vesicle (g/100 g BW)	0.26 ± 0.08	0.25 ± 0.22	0.24 ± 0.05
Prostate (g/100 g BW)	0.21 ± 0.02	0.21 ± 0.03	0.18 ± 0.03

Values are mean ± standard deviations

*, **Significantly different from the 0 mg/kg group at $p < 0.05$, 0.01, respectively

macroscopic findings in the 25 and 50 mg/kg groups. Histopathological findings of dead and moribund sacrificed animals are summarized in Table 4. Marked to severe centrilobular necrosis of hepatocytes in the liver; necrosis of olfactory, respiratory, and transitional epithelial cells in the nasal cavity; and necrosis and vacuolation of proximal tubules in the kidney were observed in the 100 mg/kg group (Fig. 3). Endocardial/epicardial hemorrhages in the heart observed only in dead animals were considered to be agonal changes. Histopathological findings of animals sacrificed at the end of the experiment are summarized in Table 5.

Table 4 Histopathology for dead/moribund sacrificed animals in a preliminary 4-week repeated dose oral toxicity study

Organs	Findings		1,3-DCP (mg/kg) 100
No. of animals examined			5 (1)
Liver	Necrosis, hepatocytes, centrilobular	+++	1 (1)
		++++	4 (0)
Nasal cavity	Necrosis, olfactory epithelium	+++	5 (1)
	Necrosis, respiratory epithelium	±	1 (0)
		+	3 (0)
	Necrosis, transitional epithelium	±	1 (0)
		+	3 (0)
Kidney	Necrosis, proximal tubule	±	1 (0)
		+	4 (1)
	Vacuolation, proximal tubule	±	5 (1)
Heart	Hemorrhage, endocardial/epicardial	+	2 (0)
		++	2 (0)

(): No. of moribund sacrificed animals

±: Minimal, +: Mild, ++: Moderate, +++: Marked, ++++: Severe

Single-cell necrosis of centrilobular hepatocytes in the liver and disarrangement and vacuolation of respiratory epithelial cells in the nasal cavity were observed in the 25 and 50 mg/kg groups (Fig. 4A and B). There were no histopathological abnormalities in the lungs and trachea in all 1,3-DCP treated animals.

Immunohistochemistry, measurement of 8-OHdG, western blotting, and qPCR in the liver

Single-cell necrosis observed in the livers of rats in the 25 and 50 mg/kg groups was positive for c-caspase 3, an apoptosis marker (Fig. 4C). The number of c-caspase 3-positive cells was significantly increased in the 50 mg/kg group with dose dependency (Fig. 4D). 8-OHdG levels were not changed in the livers of rats treated with 1,3-DCP compared with those in the control group (Fig. 4E). In immunohistochemistry for GST-P, centrilobular hepatocytes were immunoreactive for GST-P in the livers of rats treated with 25 and 50 mg/kg 1,3-DCP, whereas there were no typical preneoplastic GST-P-positive foci (Fig. 4F). The expression of GST-P was confirmed by qPCR analysis and western blotting (Fig. 4G and H). In the livers of rats in the 25 and 50 mg/kg groups, the number of Ki67-positive cells was significantly increased, and Ki67-positive cells were mainly localized in the centrilobular zone (Fig. 4I and J). In addition, mRNA expression levels of cyclin A2 in the 25 and

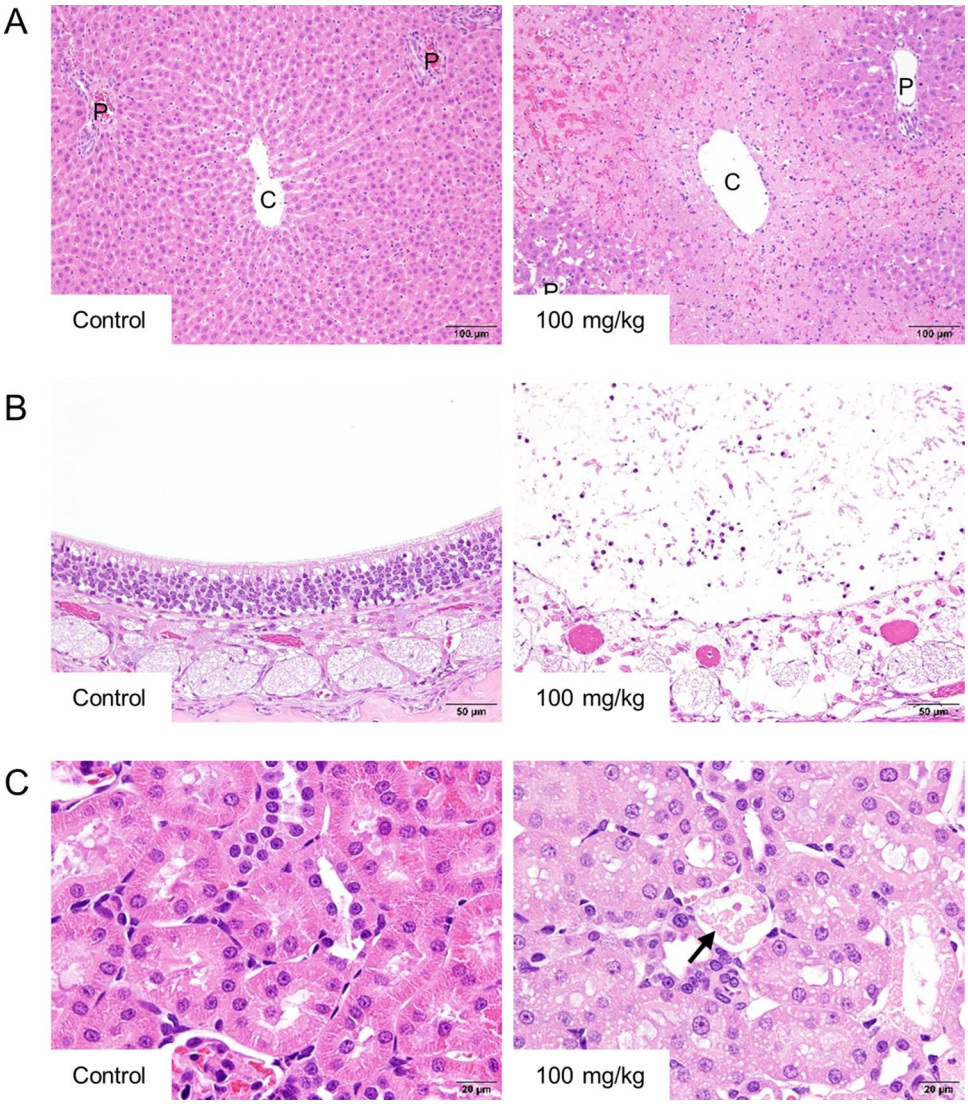

Fig. 3 Representative histopathological findings for the liver, nasal cavity, and kidneys of dead/moribund sacrificed animals treated with a single dose of 100 mg/kg 1,3-DCP. **A** Severe necrosis of hepatocytes was observed in the centrilobular zone in the livers of rats treated with 100 mg/kg 1,3-DCP. C: central vein, P: portal triad. **B** Olfactory cells in the nasal cavity of rats treated with 100 mg/kg 1,3-DCP were broadly necrotic and exfoliated. **C** In the kidneys of rats treated with 100 mg/kg, necrosis (arrow) and vacuolation of the renal tubular epithelium were observed. HE staining (**A**, **B**, and **C**)

Table 5 Histopathology for animals sacrificed at the end of the experiment in a preliminary 4-week repeated dose oral toxicity study

Organs	Findings		1,3-DCP (mg/kg)		
			0	25	50
No. of animals examined			5	5	5
Liver	Single cell necrosis, hepatocytes, centrilobular	±	2	4	–
		+	–	1	5
Nasal cavity	Disarrangement, respiratory epithelium	±	–	4	3
		+	–	–	1
	Vacuolation, respiratory epithelium	±	–	1	–
		+	–	–	2
		++	–	–	1

±: Minimal, +: Mild, ++: Moderate

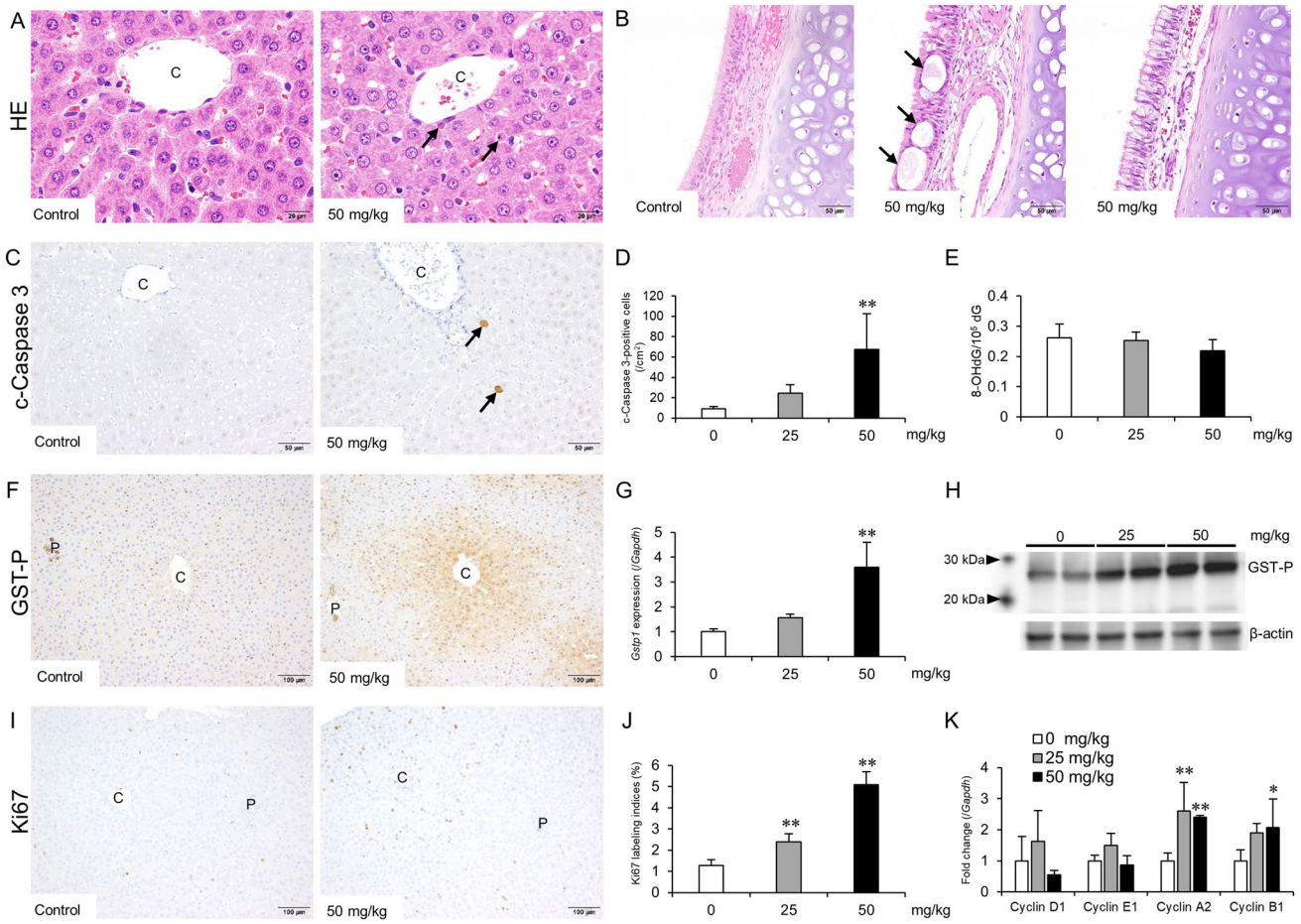

Fig. 4 Analysis of liver and nasal cavity tissues from rats in the 25 and 50 mg/kg groups in a preliminary 4-week repeated dose study. **A** Representative histopathological findings of single-cell necrosis of hepatocytes (arrows) observed in the centrilobular zone of the livers of control and 50 mg/kg groups. **B** Representative histopathological findings of disarrangement (arrows) and vacuolation of the respiratory epithelium of the nasal cavity from rats in the control and 50 mg/kg groups. **C** c-Caspase 3-positve hepatocytes (arrows) were mainly observed in the centrilobular zone in the liver of rats in the 50 mg/kg group. **D** Number of c-caspase 3-positive hepatocytes was significantly increased in the 50 mg/kg group in a dose-dependent manner. **E** There were no changes in 8-hydroxy-2′-deoxyguanosine (8-OHdG) levels in the liver following 1,3-DCP treatment. **F** Representative immunohistochemical findings for glutathione *S*-transferase placental form (GST-P). In the liver of rats in the 50 mg/kg group, centrilobular hepatocytes were positive for GST-P, whereas preneoplastic GST-P-positive foci were not observed. **G** qPCR analysis revealed that *Gstp1* mRNA was significantly upregulated in the 50 mg/kg group in a dose-dependent manner. **H** In western blotting analysis, GST-P protein (23 kDa) was upregulated in the liver of rats in the 25 and 50 mg/kg groups. **I** Representative immunohistochemical findings for Ki67. In the liver of rats in the 50 mg/kg group, Ki67-positive hepatocytes were increased mainly in the centrilobular zone. **J** Number of Ki67-positive hepatocytes was significantly increased in the liver of rats in the 25 and 50 mg/kg groups. **K** qPCR analysis showed that mRNA expression of cyclin A2 was significantly increased in the 25 and 50 mg/kg groups, whereas that of cyclin B1 was significantly increased in the 50 mg/kg group. HE staining (A and B) and immunohistochemistry for c-caspase 3 (C), GST-P (F), and Ki67 (I). *C* central vein, *P* portal triad. Values are means ± standard deviations for five rats (D, E, G, J, and K). *, **Significantly different from the control group at $p < 0.05$, 0.01, respectively

50 mg/kg groups and cyclin B1 in the 50 mg/kg group were significantly increased (Fig. 4K).

Experiment 2

In vivo mutation assay using excised liver tissues at week 6

gpt MFs were significantly increased in the livers of rats treated with 1,3-DCP and ES (Table 6). The results of analysis for *gpt* mutation spectra are shown in Table 7. GC-AT and AT-GC transitions and AT-TA transversions were significantly increased in the livers of rats treated with 1,3-DCP. ES induced significant increases in GC-TA and GC-CG transversions and AT-GC transitions, consistent with the results of previous reports (Suzuki et al. 2012).

Table 6 *gpt* mutant frequencies in the livers of F344 *gpt* delta rats treated with 1,3-DCP and estragole in the GPG model

Group	Animal no	CmR colonies ($\times 10^5$)	6-TGR and CmR colonies	Mutant frequency ($\times 10^{-5}$)	Mean ± standard deviation
Control	101	4.3	0[a]	–	0.36 ± 0.26
	102	5.0	2	0.40	
	103	5.0	1	0.20	
	104	4.5	3	0.67	
	105	5.9	1	0.17	
1,3-DCP	201	3.4	26	7.65	6.44 ± 1.17**
	202	6.2	35	5.65	
	203	3.5	26	7.43	
	204	3.8	25	6.58	
	205	5.3	26	4.91	
Estragole	301	4.9	5	1.02	2.13 ± 0.81**
	302	5.3	12	2.26	
	303	7.4	12	1.62	
	304	5.3	15	2.83	
	305	5.5	16	2.91	

[a]No mutant colonies were detected on the plate, and these data were excluded from the calculation of mutant frequency

**Significantly different from the control group at $p < 0.01$

Table 7 Mutation spectra of *gpt* mutant colonies in the liver of F344 *gpt* delta rats treated with 1,3-DCP and estragole in the GPG model

	Control		1,3-DCP		Estragole	
	No. (%)	Mutation frequency ($\times 10^{-5}$)	No. (%)	Mutation frequency ($\times 10^{-5}$)	No. (%)	Mutation frequency ($\times 10^{-5}$)
Transversion						
GC-TA	1[a] (14.3)	0.06 ± 0.11[b]	4 (2.9)	0.18 ± 0.16	10 (16.7)	0.37 ± 0.19*
GC-CG	0 (0)	0	1 (0.7)	0.06 ± 0.13	7 (11.7)	0.24 ± 0.08**
AT-TA	0 (0)	0	10 (7.2)	0.43 ± 0.33*	8 (13.3)	0.27 ± 0.21
AT-CG	0 (0)	0	3 (2.2)	0.12 ± 0.16	3 (5.0)	0.11 ± 0.17
Transition						
GC-AT	4 (57.1)	0.20 ± 0.02	84 (60.9)	3.92 ± 1.04**	11 (18.3)	0.40 ± 0.25
AT-GC	0 (0)	0	33 (23.9)	1.58 ± 0.84**	18 (30.0)	0.64 ± 0.20**
Deletion						
Single bp	1 (14.3)	0.06 ± 0.11	0 (0)	0 ± 0	0 (0)	0 ± 0
Over 2 bp	0 (0)	0	1 (0.7)	0.06 ± 0.13	0 (0)	0 ± 0
Insertion	0 (0)	0	0 (0)	0 ± 0	1 (1.7)	0.04 ± 0.08
Complex	1 (14.3)	0.05 ± 0.10	2 (1.4)	0.10 ± 0.14	2 (3.3)	0.06 ± 0.09

[a]Number of colonies with independent mutations

[b]Mean ± standard deviation

*, **Significantly different from the control group at $p < 0.05$, 0.01, respectively

Analysis of GST-P-positive foci and cell proliferative activity in residual liver tissues at week 13

Apoptosis of hepatocytes was observed in the centrilobular zone of the residual liver tissues of rats treated with 1,3-DCP (data not shown), consistent with the results of a preliminary 4-week repeated dose study. There were no significant changes in number and area of GST-P-positive foci in the livers of rats treated with 1,3-DCP compared with the control group, whereas the development of GST-P-positive foci was significantly promoted by ES treatment (Fig. 5A, B). The number of Ki67-positive hepatocytes was significantly increased by 1,3-DCP treatment, and Ki67-positive hepatocytes were mainly localized in the centrilobular zone

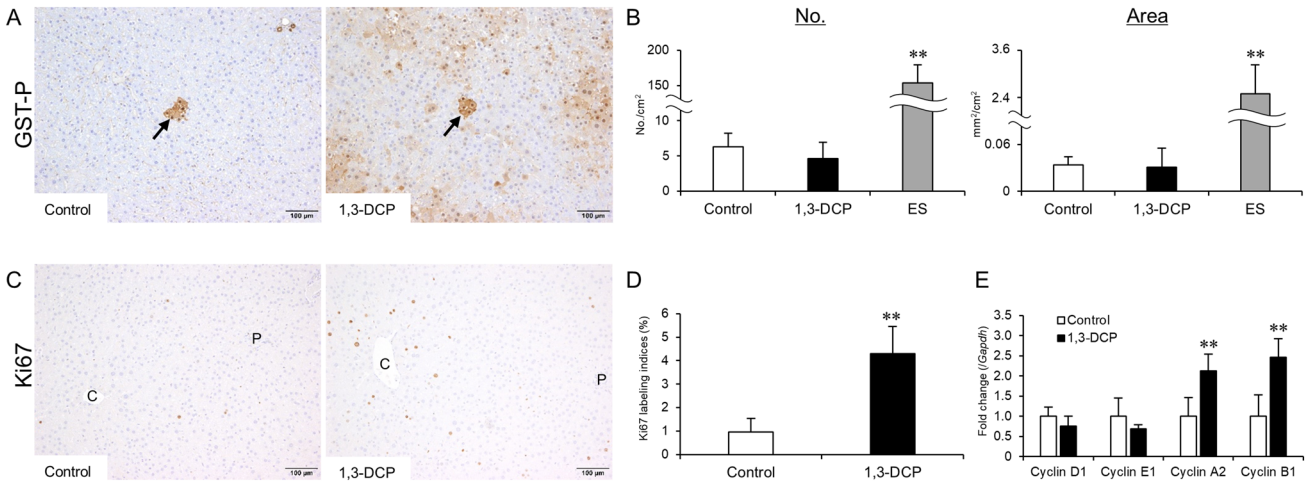

Fig. 5 Analysis of preneoplastic lesions and cell proliferative activities in residual liver tissues in the GPG model at week 13. **A** Representative immunohistochemical findings for glutathione *S*-transferase placental form (GST-P)-positive foci (arrows). **B** Number and area of GST-P-positive foci were not enhanced by 1,3-DCP treatment, whereas estragole (ES), a genotoxic hepatocarcinogen, clearly promoted the development of GST-P-positive foci. **C** Representative immunohistochemical findings for Ki67. In the liver of rats treated with 1,3-DCP, Ki67-positive hepatocytes were increased mainly in the centrilobular zone. **D** Number of Ki67-positive hepatocytes was significantly increased in the liver following 1,3-DCP treatment. **E** qPCR analysis revealed significant increases in cyclin A2 and cyclin B1 mRNA expression in the liver of rats treated with 1,3-DCP. Immunohistochemistry for GST-P (**A**) and Ki67 (**C**). *C* central vein, *P* portal triad. Values are means ± standard deviations for 15 (**B**) or five rats (**D** and **E**). **Significantly different from the control group at $p < 0.01$

(Fig. 5C, D). mRNA expression levels of cyclin A2 and cyclin B1 also showed significant increases in the livers of rats treated with 1,3-DCP (Fig. 5E).

Experiment 3

In vivo mutation assay using excised kidney tissues at week 6

gpt MFs were significantly increased in the kidneys of rats treated with 1,3-DPC and AA (Table 8). The results

Table 8 *gpt* mutant frequencies in the kidneys of F344 *gpt* delta rats treated with 1,3-DCP and aristolochic acid in the GNP model

Group	Animal no	CmR colonies ($\times 10^5$)	6-TGR and CmR colonies	Mutant frequency ($\times 10^{-5}$)	Mean ± standard deviation
Control	11	3.7	0[a]	–	0.53 ± 0.25
	12	1.7	1	0.59	
	13	4.7	2	0.43	
	14	3.8	2	0.53	
	15	3.4	2	0.59	
1,3-DCP	21	2.7	8	2.99	2.90 ± 1.18**
	22	2.3	11	4.83	
	23	3.0	6	2.02	
	24	4.0	11	2.78	
	25	3.7	7	1.89	
Aristolochic acid	31	2.8	16	5.77	3.37 ± 1.99**
	32	3.2	7	2.21	
	33	1.9	10	5.18	
	34	4.1	5	1.22	
	35	3.7	9	2.46	

[a]No mutant colonies were detected on the plate, and these data were excluded from the calculation of mutant frequency

**Significantly different from the control group at $p < 0.01$

Table 9 Mutation spectra of *gpt* mutant colonies in the kidneys of F344 *gpt* delta rats treated with 1,3-DCP and aristolochic acid in the GNP model

	Control		1,3-DCP		Aristolochic acid	
	No. (%)	Mutation frequency ($\times 10^{-5}$)	No. (%)	Mutation frequency ($\times 10^{-5}$)	No. (%)	Mutation frequency ($\times 10^{-5}$)
Transversion						
GC-TA	2[a] (28.6)	0.14 ± 0.16[b]	6 (14.0)	0.35 ± 0.34	5 (10.6)	0.40 ± 0.38
GC-CG	0 (0)	0	0 (0)	0	4 (8.5)	0.35 ± 0.49
AT-TA	0 (0)	0	3 (7.0)	0.20 ± 0.33	22 (46.8)	1.49 ± 0.66**
AT-CG	0 (0)	0	1 (2.3)	0.09 ± 0.20	2 (4.3)	0.14 ± 0.32
Transition						
GC-AT	2 (28.6)	0.12 ± 0.14	25 (58.1)	1.76 ± 1.05**	5 (10.6)	0.34 ± 0.35
AT-GC	0 (0)	0	6 (14.0)	0.36 ± 0.25*	4 (8.5)	0.31 ± 0.32
Deletion						
Single bp	1 (14.3)	0.05 ± 0.11	0 (0)	0	5 (10.6)	0.34 ± 0.21*
Over 2 bp	1 (14.3)	0.07 ± 0.15	2 (4.7)	0.14 ± 0.20	0 (0)	0
Insertion	0 (0)	0	0 (0)	0	0 (0)	0
Complex	1 (14.3)	0.15 ± 0.30	0 (0)		0 (0)	

[a]Number of colonies with independent mutations

[b]Mean ± standard deviation

*, **Significantly different from the control group at $p < 0.05$, 0.01, respectively

of analysis for *gpt* mutation spectra are shown in Table 9. GC-AT and AT-GC transitions were significantly increased in the kidneys of rats treated with 1,3-DCP. AT-TA transversions and single base pair deletions were significantly increased in the kidneys of rats treated with AA, similar to the results of a previous study (Matsushita et al. 2015).

Histopathological analysis and analysis of cell proliferative activity in residual kidney tissues at week 19

Development of atypical tubule hyperplasia was significantly enhanced in the kidneys of rats treated with 1,3-DCP and AA (Fig. 6A, B). In PAS-stained specimens, PAS-positive granules were observed in the glomerulus and epithelium of renal tubules with luminal hyaline cast in the kidneys of rats treated with 1,3-DCP (Fig. 6C, D). There were significant increases in the numbers of Ki67-positive renal cells in the kidneys of rats treated with 1,3-DCP (Fig. 6E, F). mRNA expression levels of cyclin E1 and cyclin A2 were significantly increased, and mRNA expression levels of cyclin B1 tended to increase ($p = 0.0517$) in the kidneys of rats treated with 1,3-DCP (Fig. 6G).

Discussion

The results of our 4-week repeated dose study revealed that the liver, hematopoietic system, nasal cavity tissue, and kidneys are target organs for toxicity of 1,3-DCP, consistent with the results of previous toxicity studies (NTP 2005). All animals in the 100 mg/kg group died or were moribund sacrificed after single administration. However, there were no changes in BWs and food consumption in the 25 and 50 mg/kg groups compared with those in the control group during the experimental period. Based on these data, the dosage of 1,3-DCP applied for rats in the GPG and GNP models was set at 50 mg/kg as the maximum tolerated dose. Acute liver failure due to severe necrosis of centrilobular hepatocytes was considered to be the cause of death in the 100 mg/kg group. Previous reports have shown that high exposure to 1,3-DCP induces severe hepatic injury in humans and experimental animals (Haratake et al. 1993; Katoh et al. 1998). Other studies have demonstrated that 1,3-DCP decreases glutathione *S*-transferase (GST) expression and glutathione levels, leading to reactive oxygen species production (Lee et al. 2016; Park et al. 2010). This is identical to the mechanisms of acetaminophen (APAP)-induced liver injury (Bhushan and Apte 2019). APAP also causes severe centrilobular necrosis of hepatocytes as with 1,3-DCP, suggesting that oxidative stress was involved in severe hepatocellular necrosis observed in the livers of rats in the 100 mg/kg group in the current study. By contrast, 8-OHdG levels in the livers of rats treated with 25 and 50 mg/kg 1,3-DCP were not changed, indicating that mechanisms other than oxidative DNA damage may be involved in 1,3-DCP-induced apoptosis of hepatocytes.

In our 4-week repeated dose study, absolute and relative liver weights were clearly increased without hypertrophic changes in hepatocytes in the 25 and 50 mg/kg groups (approximate increases of 27–31% for absolute weight

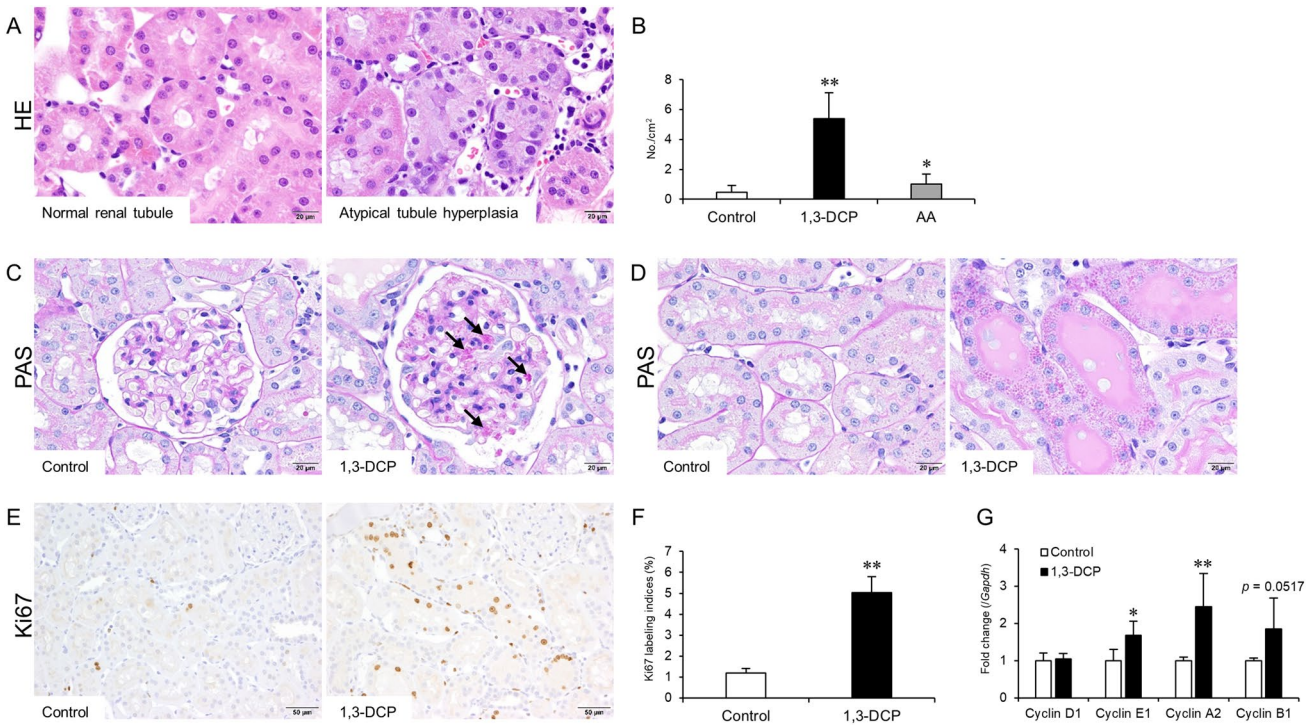

Fig. 6 Analysis of preneoplastic lesions and cell proliferative activities in residual kidney tissues from rats in the GNP model at week 19. **A** Representative photographs of normal renal tubule and atypical tubule hyperplasia. **B** Degree of atypical tubule hyperplasia was significantly increased by treatment with 1,3-DCP and aristolochic acid (AA), a genotoxic renal carcinogen. **C** Periodic Acid-Schiff (PAS)-positive granules (arrows) were deposited in the glomerulus of the kidneys of rats treated with 1,3-DCP. **D** PAS-positive granules were also observed in the epithelium of renal tubules with luminal hyaline cast. **E** Ki67-positive cells were mainly increased in renal tubular cells in the kidneys of rats treated with 1,3-DCP. **F** Ki67-positive cells were significantly increased in the kidneys following 1,3-DCP treatment. **G** In qPCR analysis, mRNA levels of cyclin E1 and cyclin A2 were significantly increased, whereas those of cyclin B1 tended to increase ($p = 0.0517$) in the kidneys following 1,3-DCP treatment. HE (**A**) and PAS (**C** and **D**) staining. Immunohistochemistry for Ki67 (**E**). Values are means ± standard deviations for 15 (**B**) or five rats (**F** and **G**). *, **Significantly different from the control group at $p < 0.05$, 0.01, respectively

and 27–34% for relative weight compared with the control). Given the increase in Ki67-positive hepatocytes and mRNA expression of cell cycle-related genes, cell proliferation was thought to contribute to the hepatomegaly observed in the current study. In the 25 and 50 mg/kg groups, a number of Ki67-positive hepatocytes and the GST-P-positive reaction were observed in centrilobular hepatocytes, whereas no development of preneoplastic foci of cellular alterations expressing GST-P was observed. Makino et al. (1998, 2008) demonstrated that 3 days of exposure to 1,2-bis(2-pyridyl)ethylene (2PY-e) and butylated hydroxyanisole (BHA) induced GST-P expression in hepatocytes with cell proliferation in the centrilobular and periportal zones, respectively. In these studies, given that BHA showed protective effects for various types of hepatocarcinogens by detoxification via induction of phase II enzymes (Buetler et al. 1995), the authors concluded that induction of GST-P was not a carcinogenic effect. GST-P is a novel preneoplastic marker in the livers of rats (Tsuda et al. 2010) and is an isoform of GST, a phase II enzyme contributing to detoxification of various carcinogens (Gajewska and Szczypka 1992). Therefore, the GST-P expression observed in the current 4-week study may be related to phase II enzyme induction rather than carcinogenicity.

In the GPG and GNP models, *gpt* MFs were clearly increased in excised liver and kidney tissues of rats treated with 1,3-DCP, strongly supporting the involvement of genotoxic mechanisms in 1,3-DCP-induced hepato- and renal carcinogenesis. Sequence analysis revealed the characteristic mutation spectra of 1,3-DCP and GC-AT and AT-GC transitions in both the liver and kidneys. Previous reports have demonstrated that the GC-AT transition was observed in *Salmonella typhimurium* TA100 treated with dichloromethane (DCM) and 1,2-dichloropropane (1,2-DCP) and in liver samples from human workers exposed to high levels of DCM and 1,2-DCP (Akiba et al. 2017; Mimaki et al. 2016). These findings implied that such transitions are characteristic mutation spectra of halogenated hydrocarbons. However, the detailed mechanisms of 1,3-DCP-induced gene

mutations remain unknown. Because epichlorohydrin, a reactive metabolite of 1,3-DCP in rats, forms adducts with hemoglobin and DNA (Landin et al. 1999; Waidyanatha et al. 2014), further investigations are currently ongoing to identify 1,3-DCP-specific DNA adducts.

In immunohistochemical analysis of GST-P in the GPG model, there were positive reactions in centrilobular hepatocytes of residual liver tissues of rats treated with 1,3-DCP. GST-P induction was thought to be related to phase II enzyme induction as with a preliminary 4-week study. By contrast, the development of GST-P-positive foci initiated by DEN was not promoted by 1,3-DCP treatment, indicating that 1,3-DCP exhibited limited tumor-promoting activity. The results of immunohistochemistry for Ki67 and qPCR analysis for cell cycle-related genes demonstrated upregulation of cell proliferative activity in residual liver tissues of rats treated with 1,3-DCP. Ki67-positive hepatocytes were mainly increased in the centrilobular zone, suggesting that cell proliferation was related to GST-P induction, consistent with previous reports (Makino et al. 1998, 2008). These findings implied that the contribution of cell proliferation associated with phase II enzyme induction to clonal expansion was limited in hepatocarcinogenesis. Overall, the data obtained from our GPG model indicated that genotoxic mechanisms were involved in 1,3-DCP-induced hepatocarcinogenesis, whereas the tumor-promoting effects of 1,3-DCP in the liver were limited.

In the GNP model, the development of atypical tubule hyperplasia initiated by DEN was promoted in the residual kidney tissues of rats treated with 1,3-DCP, indicating that 1,3-DCP enhanced clonal expansion in renal carcinogenesis. Detailed histopathological examinations revealed that there were PAS-positive granules in the glomerulus and renal tubular epithelium with luminal hyaline cast in the residual kidney tissues of rats treated with 1,3-DCP. Similar pathological changes were observed in the kidneys of rats treated with puromycin aminonucleoside, a well-known antibiotic showing glomerular toxicity in the kidneys of rats (Löwenborg et al. 2000; Rasch et al. 2002). In the damaged glomerulus, abnormal transglomerular passage of albumin and high-molecular-weight proteins to the renal tubular lumen occurs, leading to toxicity of renal tubules owing to overload of abnormally filtered proteins (D'Amico and Bazzi 2003). Cell proliferative activity of renal tubular cells is increased in both injured and uninjured nephrons to compensate for decreased renal function (Matsushita et al. 2018, 2020). In fact, the results of immunohistochemistry for Ki67 and qPCR analysis for cell cycle-related genes showed increased cell proliferative activities in the residual kidney tissues of rats treated with 1,3-DCP, which may have contributed to the tumor-promoting activity. Thus, data obtained from the GNP model suggested that 1,3-DCP exerted both genotoxic and tumor-promoting effects in the kidneys.

In conclusion, we demonstrated that genotoxic mechanisms may be involved in 1,3-DCP-induced hepato- and renal carcinogenesis. In addition, 1,3-DCP had limited tumor-promoting activity in the liver, but promoted clonal expansion in the kidneys via renal cell proliferation following glomerular injury. Overall, the data from this study provide valuable insights into the underlying mechanisms of 1,3-DCP-induced carcinogenesis and consolidate evidence for safety assessment of 1,3-DCP.

Acknowledgements We appreciate the expert technical assistance of Ms. Ayako Saikawa and Ms. Yoshimi Komatsu.

Funding This work was supported by a Grant-in-Aid from the Ministry of Health, Labour, and Welfare, Japan (grant no. H30-Syokuhin-Wakate-001).

Conflict of interests All authors declare that they have no conlicts of interest. T. Y. is an employee of Sanwa Kagaku Kenkyusho (Nagoya, Japan).

References

Akiba N, Shiizaki K, Matsushima Y, Endo O, Inaba K, Totsuka Y (2017) Influence of GSH *S*-transferase on the mutagenicity induced by dichloromethane and 1,2-dichloropropane. Mutagenesis 32:455–462. https://doi.org/10.1093/mutage/gex014

Andres S, Appel KE, Lampen A (2013) Toxicology, occurrence and risk characterisation of the chloropropanols in food: 2-monochloro-1,3-propanediol, 1,3-dichloro-2-propanol and 2,3-dichloro-1-propanol. Food Chem Toxicol 58:467–487. https://doi.org/10.1016/j.fct.2013.05.024

Bhushan B, Apte U (2019) Liver regeneration after acetaminophen hepatotoxicity: mechanisms and therapeutic opportunities. Am J Pathol 189:719–729. https://doi.org/10.1016/j.ajpath.2018.12.006

Buetler TM, Gallagher EP, Wang C, Stahl DL, Hayes JD, Eaton DL (1995) Induction of phase I and phase II drug-metabolizing enzyme mRNA, protein, and activity by BHA, ethoxyquin, and oltipraz. Toxicol Appl Pharmacol 135:45–57. https://doi.org/10.1006/taap.1995.1207

D'Amico G, Bazzi C (2003) Pathophysiology of proteinuria. Kidney Int 63:809–825. https://doi.org/10.1046/j.1523-1755.2003.00840.x

Frazier KS, Seely JC, Hard GC, Betton G, Burnett R, Nakatsuji S, Nishikawa A, Durchfeld-Meyer B, Bube A (2012) Proliferative and nonproliferative lesions of the rat and mouse urinary system. Toxicol Pathol 40:14S-86S. https://doi.org/10.1177/0192623312438736

Gajewska J, Szczypka M (1992) Role of pi form of glutathione *S*-transferase (GST-pi) in cancer: a minireview. Mater Med Pol 24:45–49

Haratake J, Furuta A, Iwasa T, Wakasugi C, Imazu K (1993) Submassive hepatic necrosis induced by dichloropropanol. Liver 13:123–129. https://doi.org/10.1111/j.1600-0676.1993.tb00618.x

Hibi D, Yokoo Y, Suzuki Y, Ishii Y, Jin M, Kijima A, Nohmi T, Nishikawa A, Umemura T (2017) Lack of genotoxic mechanisms in early-stage furan-induced hepatocellular tumorigenesis in *gpt* delta rats. J Appl Toxicol 37:142–149. https://doi.org/10.1002/jat.3331

Ishii Y, Kijima A, Takasu S, Ogawa K, Umemura T (2019a) Effects of inhibition of hepatic sulfotransferase activity on renal

genotoxicity induced by lucidin-3-*o*-primeveroside. J Appl Toxicol 39:650–657. https://doi.org/10.1002/jat.3755

Ishii Y, Yokoo Y, Kijima A, Takasu S, Ogawa K, Umemura T (2019b) DNA modifications that do not cause gene mutations confer the potential for mutagenicity by combined treatment with food chemicals. Food Chem Toxicol 129:144–152. https://doi.org/10.1016/j.fct.2019.04.011

Jin M, Kijima A, Hibi D, Ishii Y, Takasu S, Matsushita K, Kuroda K, Nohmi T, Nishikawa A, Umemura T (2013) In vivo genotoxicity of methyleugenol in *gpt* delta transgenic rats following medium-term exposure. Toxicol Sci 131:387–394. https://doi.org/10.1093/toxsci/kfs294

Joint FAO/WHO Expert Committee on Food Additives (2006) Technical Report Series 940

Katoh T, Haratake J, Nakano S, Kikuchi M, Yoshikawa M, Arashidani K (1998) Dose-dependent effects of dichloropropanol on liver histology and lipid peroxidation in rats. Ind Health 36:318–323. https://doi.org/10.2486/indhealth.36.318

Landin HH, Segerbäck D, Damberg C, Osterman-Golkar S (1999) Adducts with haemoglobin and with DNA in epichlorohydrin-exposed rats. Chem Biol Interact 117:49–64. https://doi.org/10.1016/s0009-2797(98)00099-4

Lee IC, Lee SM, Ko JW, Park SH, Shin IS, Moon C, Kim SH, Kim JC (2016) Role of mitogen-activated protein kinases and nuclear factor-kappa b in 1,3-dichloro-2-propanol-induced hepatic injury. Lab Anim Res 32:24–33. https://doi.org/10.5625/lar.2016.32

Löwenborg EK, Jaremko G, Berg UB (2000) Glomerular function and morphology in puromycin aminonucleoside nephropathy in rats. Nephrol Dial Transplant 15:1547–1555. https://doi.org/10.1093/ndt/15.10.1547

Makino T, Sehata S, Igarashi I, Watanabe T, Ohashi Y, Manabe S, Yamoto T (1998) Induction of glutathione *S*-transferases and hepatocellular proliferating activites in the rat liver treated with tret-butylated hydroxyanisole, 1, 2-bis(2-pyridyl)ethylene, and phenobarbial. J Toxicol Pathol 11:183–189

Makino T, Ishikawa K, Igarashi I, Yamoto T, Manabe S, Nakayama H (2008) Relationship between GST Yp induction and hepatocyte proliferation in rats treated with phase II drug metabolizing enzyme inducers. Toxicol Pathol 36:420–427. https://doi.org/10.1177/0192623308315359

Matsushita K, Kijima A, Ishii Y, Takasu S, Jin M, Kuroda K, Kawaguchi H, Miyoshi N, Nohmi T, Ogawa K, Umemura T (2013) Development of a medium-term animal model using *gpt* delta rats to evaluate chemical carcinogenicity and genotoxicity. J Toxicol Pathol 26:19–27. https://doi.org/10.1293/tox.26.19

Matsushita K, Kuroda K, Ishii Y, Takasu S, Kijima A, Kawaguchi H, Miyoshi N, Nohmi T, Ogawa K, Nishikawa A, Umemura T (2014) Improvement and validation of a medium-term *gpt* delta rat model for predicting chemical carcinogenicity and underlying mode of action. Exp Toxicol Pathol 66:313–321. https://doi.org/10.1016/j.etp.2014.05.002

Matsushita K, Ishii Y, Takasu S, Kuroda K, Kijima A, Tsuchiya T, Kawaguchi H, Miyoshi N, Nohmi T, Ogawa K, Nishikawa N, Umemura T (2015) A medium-term *gpt* delta rat model as an in vivo system for analysis of renal carcinogenesis and the underlying mode of action. Exp Toxicol Pathol 67:31–39. https://doi.org/10.1016/j.etp.2014.09.006

Matsushita K, Takasu S, Kuroda K, Ishii Y, Kijima A, Ogawa K, Umemura T (2018) Mechanisms underlying exacerbation of osmotic nephrosis caused by pre-existing kidney injury. Toxicol Sci 165:420–430. https://doi.org/10.1093/toxsci/kfy151

Matsushita K, Toyoda T, Yamada T, Morikawa T, Ogawa K (2020) Comprehensive expression analysis of mRNA and microRNA for the investigation of compensatory mechanisms in the rat kidney after unilateral nephrectomy. J Appl Toxicol 40:1373–1383. https://doi.org/10.1002/jat.3990

Mimaki S, Totsuka Y, Suzuki Y, Nakai C, Goto M, Kojima M, Arakawa H, Takemura S, Tanaka S, Marubashi S, Kinoshita M, Matsuda T, Shibata T, Nakagama H, Ochiai A, Kubo S, Nakamori S, Esumi H, Tsuchihara K (2016) Hypermutation and unique mutational signatures of occupational cholangiocarcinoma in printing workers exposed to haloalkanes. Carcinogenesis 37:817–826. https://doi.org/10.1093/carcin/bgw066

National Toxicology Programs (2005) Review of Toxicological Literature, 1,3-Dichloro-2-propanol (CAS No. 96-23-1). https://ntp.niehs.nih.gov/ntp/htdocs/chem_background/exsumpdf/dichloropropanol_508.pdf

Nohmi T (2016) Past, present and future directions of *gpt* delta rodent gene mutation assays. Food Saf (tokyo) 4:1–13. https://doi.org/10.14252/foodsafetyfscj.2015024

Nohmi T, Suzuki T, Masumura K (2000) Recent advances in the protocols of transgenic mouse mutation assays. Mutat Res 455:191–215. https://doi.org/10.1016/s0027-5107(00)00077-4

Park SY, Kim YH, Kim YH, Lee SJ (2010) 1,3-dichloro-2-propanol induces apoptosis via both calcium and ROS in mouse melanoma cells. Biotechnol Lett 32:45–51. https://doi.org/10.1007/s10529-009-0117-z

Rasch R, Nyengaard JR, Marcussen N, Meyer TW (2002) Renal structural abnormalities following recovery from acute puromycin nephrosis. Kidney Int 62:496–506. https://doi.org/10.1046/j.1523-1755.2002.00481.x

Suzuki Y, Umemura T, Ishii Y, Hibi D, Inoue T, Jin M, Sakai H, Kodama Y, Nohmi T, Yanai T, Nishikawa A, Ogawa K (2012) Possible involvement of sulfotransferase 1A1 in estragole-induced DNA modification and carcinogenesis in the livers of female mice. Mutat Res 749:23–28. https://doi.org/10.1016/j.mrgentox.2012.07.002

Tsuda H, Futakuchi M, Fukamachi K, Shirai T, Imaida K, Fukushima S, Tatematsu M, Furukawa F, Tamano S, Ito N (2010) A medium-term, rapid rat bioassay model for the detection of carcinogenic potential of chemicals. Toxicol Pathol 38:182–187. https://doi.org/10.1177/0192623309356451

Umemura T, Kai S, Hasegawa R, Kanki K, Kitamura Y, Nishikawa A, Hirose M (2003) Prevention of dual promoting effects of pentachlorophenol, an environmental pollutant, on diethylnitrosamine-induced hepato- and cholangiocarcinogenesis in mice by green tea infusion. Carcinogenesis 24:1105–1109. https://doi.org/10.1093/carcin/bgg053

Umemura T, Kanki K, Kuroiwa Y, Ishii Y, Okano K, Nohmi T, Nishikawa A, Hirose M (2006) In vivo mutagenicity and initiation following oxidative DNA lesion in the kidneys of rats given potassium bromate. Cancer Sci 97:829–835. https://doi.org/10.1111/j.1349-7006.2006.00248.x

Waidyanatha S, Gaudette NF, Hong Y, Fennell TR (2014) Formation of epichlorohydrin, a known rodent carcinogen, following oral administration of 1,3-dichloro-2-propanol in rats. Chem Res Toxicol 27:1787–1795. https://doi.org/10.1021/tx500239q

Williams G, Leblanc JC, Setzer RW (2010) Application of the margin of exposure (MOE) approach to substances in food that are genotoxic and carcinogenic: example: (CAS no. 96-23-1) 1,3-dichloro-2-propanol (DCP). Food Chem Toxicol 48:S57–S62. https://doi.org/10.1016/j.fct.2009.10.038